# Charged and rotating boson stars in five-dimensional Einstein-Maxwell-Chern-Simons theory

Yves Brihaye[1] and Betti Hartmann[2]

[1]*Physique de l'Univers-Champs et Gravitation, Université de Mons, 7000 Mons, Belgium*
[2]*Department of Mathematics, University College London, Gower Street, London WC1E 6BT, United Kingdom*

(Received 10 May 2023; accepted 12 June 2023; published 30 June 2023)

We study charged and rotating boson stars in five-dimensional Einstein-Maxwell-Chern-Simons theory assuming the two angular momenta associated with the two orthogonal planes of rotation to be equal. Next to the angular momenta, the boson stars carry an electric charge and a magnetic moment. Interestingly, we find new branches of Einstein-Maxwell-Chern-Simons solutions for which the spatial part of the gauge potential possesses nodes. Consequently, the magnetic moment and the gyromagnetic ratio have opposite signs as compared to the solutions on the main branch. For sufficiently large energy density we find that the solutions possess ergoregions.

DOI: 10.1103/PhysRevD.107.124060

## I. INTRODUCTION

With general relativity now the accepted and experimentally well-confirmed paradigm to describe the gravitational interaction for a wide range of masses and sizes of objects, it remains to be understood how strong gravity acts on scales where quantum effects play an important role. While a consistent theory of quantum gravity that would also be able to explain a number of puzzles, such as that of dark energy, has not been formulated so far, there are possibilities to test strong gravity in settings that could be connected to quantum theory. One such possibility is the boson star [1–6], which is made of a scalar field that is essentially quantum in nature as its collapse is prevented by Heisenberg's uncertainty relation. One could think of such a star as a "macroscopic Bose-Einstein condensate" that is self-gravitating. These solutions exist due to a global $U(1)$ symmetry of the model, which leads to a conserved Noether charge that can be interpreted as the number of scalar bosonic particles making up the star. These solitonic objects are stationary as they possess a harmonic time dependence, in their simplest version; however, they have a static energy density that leads to a static space-time. Boson stars can also rotate (with resulting stationary space-time) [2–6], and interestingly, the resulting angular momentum is given as an integer multiple of the Noether charge. Hence, the angular momentum is quantized—a feature that is very common in quantum physics—and is proportional to the total number of scalar bosonic particles that make up the star. It has been argued in [7] that boson stars with large angular momentum possess an ergoregion which would eventually make them unstable.

Gauging the $U(1)$ symmetry leads to charged boson stars [8–10]. The nonrotating boson stars possess electric charge proportional to the Noether charge, with the proportionality constant equal to the gauge coupling. These solutions exist as long as the electromagnetic repulsion does not overcome the gravitational attraction [8]; i.e., a critical value of the gauge coupling exists at fixed gravitational coupling. Adding rotation leads to solutions with electric charge and magnetic moments [11,12]. It was shown in [12] that the relation between angular momentum and Noether charge present in the uncharged case also holds in the presence of a $U(1)$ gauge field.

Boson stars can also be constructed in higher space-time dimensions, which requires a complex scalar field doublet [13]. In five space-time dimensions, rotating stars can possess two angular momenta. Choosing these two angular momenta to be equal, the symmetry of the system can be enhanced and the space-time possesses hyperspherical symmetry. As for boson stars in four space-time dimensions, the sum of the angular momenta is proportional to the Noether charge. One aim of this paper is to add a $U(1)$ gauge field to the model discussed in [13]. As we show below, these solutions possess electric charge and magnetic moments. Next to the standard Maxwell term, another possibility exists in odd space-time dimensions: a Chern-Simons gauge field interaction. While the former is a relativistic gauge field model, the Chern-Simons term is topological and does not depend on the metric. The latter is

important when building models describing phenomena in nonrelatistic physics such as, e.g., condensed matter. Charged black holes without scalar fields in Einstein-Maxwell-Chern-Simons theory have been studied in [14–17], while five-dimensional, charged, rotating black holes with scalar hair have been studied in [18]. Here, we construct the globally regular counterparts to these black holes and extend the results to include a Chern-Simons term.

Our paper is organized as follows: In Sec. II with discuss the model, while Sec. III contains our numerical results. We conclude in Sec. IV.

## II. THE MODEL

The action of the model that we consider reads

$$S=\int\left[\frac{\mathcal{R}}{16\pi G}-(D_\mu\Phi)^\dagger(D^\mu\Phi)-U(|\Phi|)-\frac{1}{4}F_{\mu\nu}F^{\mu\nu}+\alpha\frac{1}{\sqrt{-g}}\epsilon^{\mu\nu\rho\sigma\theta}A_\mu F_{\nu\rho}F_{\sigma\theta}\right]\sqrt{-g}\mathrm{d}^5x. \tag{1}$$

This is a $U(1)$ gauge field model coupled minimally to a complex scalar doublet $\Phi=(\phi_1,\phi_2)^T$ with potential $V(|\Phi|)$ as well as Einstein gravity with $\mathcal{R}$ the Ricci scalar and $G$ Newton's constant. Note that the scalar sector possesses a global $U(2)$ symmetry whose $U(1)$ subgroup can be gauged. Here, the diagonal part of the $U(1)\times U(1)$ maximal Abelian subgroup is gauged. The covariant derivative and $U(1)$ field strength tensor then take the form

$$D_\mu=(\partial_\mu-iqA_\mu),\qquad F_{\mu\nu}=\partial_\mu A_\nu-\partial_\nu A_\mu, \tag{2}$$

and $q$ denotes the gauge coupling constant. We assume $q>0$ without loss of generality since the sign of $q$ can be absorbed in the gauge fields and the Chern-Simons coupling $\alpha$. The variation of the action (1) with respect to the metric leads to the Einstein equation:

$$G_{\mu\nu}=R_{\mu\nu}-\frac{1}{2}g_{\mu\nu}R=8\pi G(T^s_{\mu\nu}+T^v_{\mu\nu}) \tag{3}$$

with the stress-energy tensor of the scalar field

$$T^s_{\mu\nu}=(D_\mu\Phi)^\dagger(D_\nu\Phi)+(D_\nu\Phi)^\dagger(D_\mu\Phi)-\frac{1}{2}g_{\mu\nu}[(D_\alpha\Phi)^\dagger(D_\beta\Phi)+(D_\beta\Phi)^\dagger(D_\alpha\Phi)]g^{\alpha\beta}-g_{\mu\nu}U(|\Phi|), \tag{4}$$

and the stress-energy tensor of the gauge field

$$T^v_{\mu\nu}=-F_{\mu\alpha}F^\alpha_\nu+\frac{1}{4}g_{\mu\nu}F_{\alpha\beta}F^{\alpha\beta}, \tag{5}$$

respectively. The variation with respect to the matter fields leads to the equations for the scalar field and gauge field, respectively,

$$\frac{1}{\sqrt{-g}}D_\mu(\sqrt{-g}D^\mu\Phi)=\frac{\partial U}{\partial|\Phi|^2}\Phi,\qquad \frac{1}{\sqrt{-g}}\partial_\mu\sqrt{-g}F^{\mu\nu}=J^\nu+3\alpha\epsilon^{\nu\rho\sigma\theta\alpha}F_{\rho\sigma}F_{\theta\alpha}, \tag{6}$$

with the five-current given by

$$J^\nu=iq((D^\nu\Phi)^\dagger\Phi-\Phi^\dagger(D^\nu\Phi)). \tag{7}$$

Note that the action (1) is invariant under a local $U(1)$ transformation up to a divergence; i.e., the equations of motion (6) are gauge invariant.

### A. The Ansatz

For the vanishing gauge field 1-form $A_\mu\mathrm{d}x^\mu=0$, the model with action (1) was first studied in [13]. We will extend these results here to include electric charge and magnetic moments as well as to study the influence of the Chern-Simons term.

As mentioned above, we assume the solutions possess bi-azimuthal symmetry, implying the existence of three commuting Killing vectors, $\xi=\partial_t$, $\eta_1=\partial_{\varphi_1}$, and $\eta_2=\partial_{\varphi_2}$. A suitable metric Ansatz then reads

$$\begin{aligned}\mathrm{d}s^2=&-b(r)\mathrm{d}t^2+\frac{\mathrm{d}r^2}{f(r)}+R(r)\mathrm{d}\theta^2\\&+h(r)\sin^2\theta(\mathrm{d}\varphi_1-W(r)\mathrm{d}t)^2\\&+h(r)\cos^2\theta(\mathrm{d}\varphi_2-W(r)\mathrm{d}t)^2\\&+(R(r)-h(r))\sin^2\theta\cos^2\theta(\mathrm{d}\varphi_1-\mathrm{d}\varphi_2)^2\end{aligned} \tag{8}$$

where $\theta\in[0,\pi/2]$, $(\varphi_1,\varphi_2)\in[0,2\pi]$, and $r$ and $t$ denote the radial and time coordinates, respectively.

For such solutions the isometry group is enhanced from $\mathbb{R}\times U(1)^2$ to $\mathbb{R}\times U(2)$. In other words, the two angular momenta $J_1, J_2$ associated with rotations by $\varphi_i$, $i=1,2$ are equal to each other, $J_1=J_2\equiv J/2$, where $J$ is the total angular momentum. The symmetry enhancement mentioned above, in particular, allows us to factorize the angular dependence and thus leads to ordinary differential equations. The Ansatz for the scalar field then reads [13]

$$\Phi=\phi(r)e^{i\omega t}\begin{pmatrix}\sin\theta e^{i\varphi_1}\\ \cos\theta e^{i\varphi_2}\end{pmatrix}, \tag{9}$$

where the frequency $\omega$ parametrizes the harmonic time dependence. For the scalar field potential we restrict our study to the simplest case of a massive, non-self-interacting scalar field; i.e., we set

$$U(|\Phi|)=\mu^2\Phi^\dagger\Phi=\mu^2\phi(r)^2 \tag{10}$$

where $\mu$ corresponds to the scalar field mass.

Finally, the Ansatz for the electromagnetic potential is chosen as

$$A_\mu \mathrm{d}x^\mu = V(r)\mathrm{d}t + A(r)(\sin^2(\theta)\mathrm{d}\varphi_1 + \cos^2(\theta)\mathrm{d}\varphi_2) \quad (11)$$

which turns out to be consistent with the symmetries of the metric and scalar fields. The nonvanishing components of the field strength tensor are then

$$F_{rt} = \frac{\mathrm{d}V(r)}{\mathrm{d}r}, \quad F_{r\varphi_1} = \frac{\mathrm{d}A(r)}{\mathrm{d}r}\sin^2\theta,$$
$$F_{r\varphi_2} = \frac{\mathrm{d}A(r)}{\mathrm{d}r}\cos^2\theta, \quad F_{\theta\varphi_1} = -F_{\theta\varphi_2} = A(r)\sin(2\theta); \quad (12)$$

i.e., our solutions possess electric and magnetic fields.

Without fixing a metric gauge, a straightforward computation leads to the following reduced action for the system:

$$\mathcal{S}_{\mathrm{eff}} = \int \mathrm{d}r\mathrm{d}t\, L_{\mathrm{eff}}, \quad \text{with}$$
$$L_{\mathrm{eff}} = L_g + 16\pi G(L_s + L_v + \alpha L_{cs}), \quad (13)$$

$$L_g = \sqrt{\frac{fh}{b}}\left(b'R' + \frac{R}{2h}b'h' + \frac{b}{2R}R'^2 + \frac{b}{h}R'h' + \frac{1}{2}RhW'^2 + \frac{2b}{f}\left(4 - \frac{h}{R}\right)\right), \quad (14)$$

$$L_s = R\sqrt{\frac{bh}{f}}\left[f\phi'^2 + \left(\frac{2}{R} + \frac{(1-qA)^2}{h} - \frac{(\omega - W + q(V+WA))^2}{b} + \mu^2\right)\phi^2\right], \quad (15)$$

$$L_v = R\sqrt{\frac{bh}{f}}\left(\frac{2A^2}{R^2} + \frac{f}{2h}(A')^2 - \frac{f}{2b}(V' + WA')^2\right), \quad (16)$$

$$L_{CS} = 16A(A'V - AV'), \quad (17)$$

with the effective gravity ($g$), scalar field ($s$), gauge field ($v$), and Chern-Simons (CS) Lagrangian density, respectively. Here and in the following, the prime denotes the derivative with respect to $r$. The equations of motion can then be consistently obtained from this reduced action by varying with respect to $h$, $b$, $f$, $R$, $W$, $F$, $V$, and $A$. Note that the effective CS Lagrangian density does not depend on the metric functions and hence will not source the spacetime curvature.

The metric gauge freedom can be fixed afterwards, leading to a system of seven independent equations plus a constraint which is a consequence of the other equations. For the construction of the solutions, we have fixed the metric gauge by taking

$$R(r) = r^2 \quad (18)$$

consistently with the standard analytic form of the Myers-Perry solution [19]. Appropriate combinations of the equations can be used such that the equation for $f(r)$ is first order while the equations of the six other functions are second order. We hence need a total of 13 conditions at $r = 0$ and/or at $r = \infty$ to specify a boundary value problem.

### B. Asymptotic behavior and boundary conditions

Boson stars are globally regular solutions. At $r = 0$ we impose the following boundary conditions:

$$f(0) = 1, \quad b'(0) = 0, \quad h(0) = 0,$$
$$W'(0) = 0, \quad V(0) = 0, \quad A(0) = 0,$$
$$A'(0) = 0, \quad \phi(0) = 0. \quad (19)$$

Note that the condition $V(0) = 0$ does not result from the requirement of regularity, but it is a choice. This choice can be made without losing generality since the equations depend only on the combination $qV + \omega$.

Moreover, we want the solutions to be asymptotically flat; i.e., we require

$$b(r) = 1 + \frac{\mathcal{M}}{r^2} + \ldots, f(r) = 1 + \frac{\mathcal{M}}{r^2} + \ldots, h(r) = r^2 + \frac{\mathcal{V}}{r^2} + \ldots, W(r) = \frac{\mathcal{J}}{r^4} + \ldots$$
$$V(r) = V_\infty + \frac{q_e}{r^2} + \ldots, A(r) = \frac{q_m}{r^2} + \ldots \phi(r) = c_0\frac{e^{-r\sqrt{\mu^2 - (\omega - qV_\infty)^2}}}{r^{3/2}} + \ldots, \quad (20)$$

where $\mathcal{M}$, $\mathcal{V}$, $\mathcal{J}$, $q_e$, $q_m$, $V_\infty$, and $c_0$ are free parameters that can only be computed from the numerical solution.

Note that the asymptotic behavior of the scalar field tells us that it acquires an effective mass $m_{\mathrm{eff}}$ with

$$m_{\mathrm{eff}}^2 \equiv \mu^2 - (\omega - qV_\infty)^2 = (\mu - \omega + qV_\infty)(\mu + \omega - qV_\infty). \quad (21)$$

The parameter $V_\infty$, i.e., the value of the electric potential $V(r)$ at $r \to \infty$, turns out to be negative in our numerical calculations. Since $V(0) = 0$, the value of $V_\infty$ corresponds to the potential difference between the origin and infinity. With the choice $q \geq 0$, this tells us that the first factor on the right-hand side of (21), which we define as

$$\Omega := \mu - \omega + qV_\infty, \quad (22)$$

determines whether the boson star is exponentially localized. Obviously, we need $\Omega \geq 0$. For $(\omega - qV_\infty)^2 \geq \mu^2$

we are above the threshold of producing scalar particles of mass $\mu$.

### C. Physical quantities

Before we discuss the relevant physical quantities of the solutions and how they can be extracted from the numerical results that we obtain, let us remark that although there are *a priori* three (four) parameters to be varied in the Maxwell (respectively, Chern-Simons) case, Newton's constant $G$ and the mass $\mu$ of the scalar field can be set to unity without loss of generality. This is achieved by a suitable rescaling of the matter fields and the coordinate $r$. Thus, we are left with the gauge coupling $q$ in the Maxwell case and, additionally, with $\alpha$ in the Maxwell-Chern-Simons case.

The mass $M$ and total angular momentum $J = J_1 + J_2$ of the solutions have been discussed in [13]. Hence, we just state the expressions here without explicitly deriving them. They read

$$M = -\frac{3\pi}{8G}\mathcal{M}, \qquad J = \frac{\pi}{4G}\mathcal{J}, \tag{23}$$

where $\mathcal{M}$ and $\mathcal{J}$ are given in (20).

Since the model we are discussing here possesses a global $U(1)$ symmetry, there exists an associated locally conserved Noether current. This is the current given in (7). The globally conserved Noether charge is then

$$Q = \int \sqrt{-g} J^0 \mathrm{d}^4x = qN \quad \text{with}$$

$$N = 2\pi^2 \int_0^\infty r^3 \sqrt{\frac{h}{fb}}(\omega + W - q(V + AW))\phi^2 \mathrm{d}r. \tag{24}$$

Note that $N$ can then be interpreted as the total number of bosonic particles making up the boson star, and $Q$ is the total charge of $N$ individual particles that each carry charge $q$. Also note that there is a relation between the angular momentum $J$ and $N$ given by [13]

$$|J| = N. \tag{25}$$

We can also define the electric charge $Q_e$ and the magnetic moment $Q_m$, respectively, as follows:

$$Q_e = \frac{\pi}{G} q_e, \qquad Q_m = \frac{\pi}{G} q_m, \tag{26}$$

where $q_e$ and $q_m$ are given in (20). Using Eq. (6) it can be shown that $Q = Q_e$, as expected. In the numerical calculation the validity of this equality is a good cross-check. Finally, the gyromagnetic ratio $\gamma$ of our solutions reads

$$\gamma = \frac{2MQ_m}{Q_e J} = \frac{2Mq_m}{q_e J}. \tag{27}$$

We also need the Ricci scalar $\mathcal{R}$ in the following. This reads

$$\mathcal{R}(r) = -f\left(\frac{b''}{b} + \frac{h''}{h} + \frac{2R''}{R}\right) + \frac{f}{2}\left(\frac{(b')^2}{b^2} + \frac{(h')^2}{h^2} + \frac{(R')^2}{R^2} + \frac{h}{b}(W')^2\right) + -\frac{R'}{Rbh}(fbh)' - \frac{1}{2bh}(f'bh' + f'b'h + fb'h') + \frac{2}{R^2}(4R - h). \tag{28}$$

We will see in the discussion of the numerical results that some configurations reach limiting solutions with $b(0) \to 0$ [while $b''(0)$ is finite], suggesting that the scalar curvature at the origin diverges for these solutions.

## III. NUMERICAL RESULTS

Due to the nonlinearity of the field equations, we have solved the equations numerically using the collocation solver COLSYS [20]. The obtained solutions typically have an accuracy of $10^{-6}$. With appropriate rescalings of the fields and coordinates, we can set $8\pi G \equiv 1$, $\mu \equiv 1$; i.e., the only two parameters to vary in the following are $q$ and $\alpha$.

### A. Einstein-Maxwell (EM) boson stars

Let us first discuss the solutions in the absence of the Chern-Simons interaction, i.e., for $\alpha = 0$.

As a cross-check of our numerics and to emphasize the changes that the presence of the gauge field brings to the model, let us briefly discuss the case $q = 0$ that has been studied in detail in [13]. We have constructed uncharged, rotating boson star solutions and studied their properties by varying the parameter $\phi'(0)$. For $\phi'(0) = 0$ the scalar field is trivial, $\phi(r) \equiv 0$, $\omega = 1$, and the space-time is simply five-dimensional Minkowski space-time. Note, however, that the limit $\phi'(0) \to 0$ is subtle: While the scalar function $\phi(r)$ becomes trivial, the mass $M$ and Noether charge $N$ do

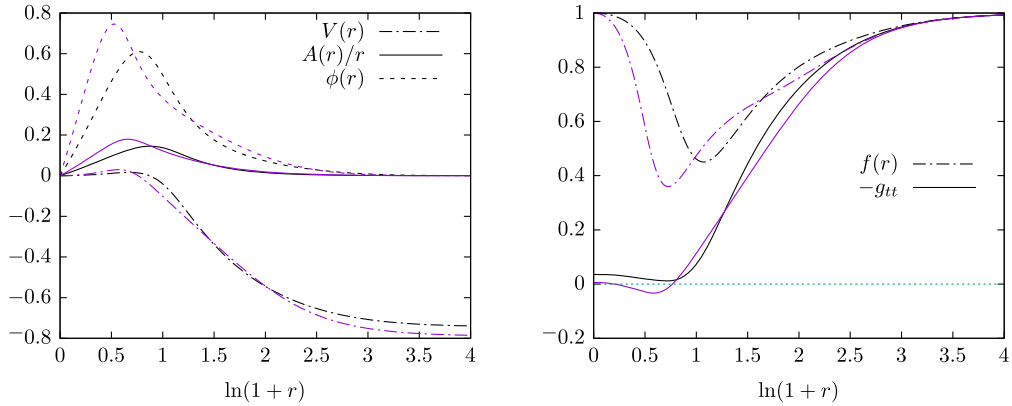


FIG. 1. Profiles of the matter field functions $V(r)$, $A(r)/r$, $\phi(r)$ (left) as well as of the metric functions $f(r)$ and $-g_{tt}$ (right) for two typical Einstein-Maxwell solutions, here for $q = 0.5$ and $\phi'(0) = 0.8$ (black) and $\phi'(0) = 1.6$ (violet), respectively.

not approach zero in this limit. In fact, a mass gap forms. This has been discussed in [13].

In Fig. 1 we show the profiles of the matter field functions $V(r)$, $A(r)/r$, $\phi(r)$ (left) as well as of the metric functions $f(r)$ and $-g_{tt}$ (right) for two typical solutions, here for $q = 0.5$ and $\phi'(0) = 0.8$ (black) and $\phi'(0) = 1.6$ (violet), respectively. This demonstrates that when increasing $\phi'(0)$, the maximal value of the scalar field function $\phi(r)$ increases and shifts to smaller values of $r$. This is very similar to $A(r)/r$. Moreover, the value of $r$ where $V(r) = 0$ shifts to smaller values of $r$. This suggested that the solution becomes more compact when increasing $\phi'(0)$. This is also confirmed by the decrease of the minimal value of $f(r)$. We also find that $-g_{tt}$ is positive for all $r$ when choosing $\phi'(0) = 0.8$; however, there exists an interval in $r$ for which $-g_{tt} < 0$ when $\phi'(0) = 1.6$, suggesting the existence of an ergoregion. We will discuss this in more detail below.

In Fig. 2 (left) we show the dependence of the mass $M$ on $\Omega$ for $q = 0$, $q = 0.25$, and $q = 0.5$, respectively. For all values of $q$ we observe the typical spiraling behavior, i.e., the existence of a main branch of solutions which exists between $\Omega = 0$ and a maximal value of $\Omega = \Omega_{\mathrm{max},1}$. From $\Omega_{\mathrm{max},1}$ a second branch of solutions extends backwards in $\Omega$ down to $\Omega_{\mathrm{min},2} > 0$. From $\Omega_{\mathrm{min},2}$ a third branch exists up to $\Omega_{\mathrm{max},3} < \Omega_{\mathrm{max},1}$ and bends backwards into a fourth branch. We find that $\Omega = \Omega_{\mathrm{max},1}, \Omega_{\mathrm{min},2}, \Omega_{\mathrm{max},3}$ all decrease with increasing $q$; i.e., the interval in $\Omega$ for which charged, rotating boson stars exist in five dimensions decreases with increasing $q$. Moreover, we find that the mass gap described above for uncharged solutions also exists for charged solutions and increases with increasing $q$. In fact, we observe that the mass range for which charged boson stars exist changes only slightly when increasing $q$ from zero to $q = 0.25$, while the increase to $q = 0.5$ increases the value of the mass gap considerably. This is related to the increased electromagnetic repulsion. The charge $Q$ and the angular momentum $J$ have a very similar qualitative dependence, which is why we do not show them here.

Along the branches, the parameter $\phi'(0)$ increases. We show the dependence of $\Omega$ on $\phi'(0)$ for $q = 0$, $q = 0.25$, and $q = 0.5$ in Fig. 2 (right). For $\phi'(0) = 0$ we have $\Omega = 0$ independent of the choice of $q$. Increasing $\phi'(0)$ the value of $\Omega$ reaches a maximal value; then, it decreases to a

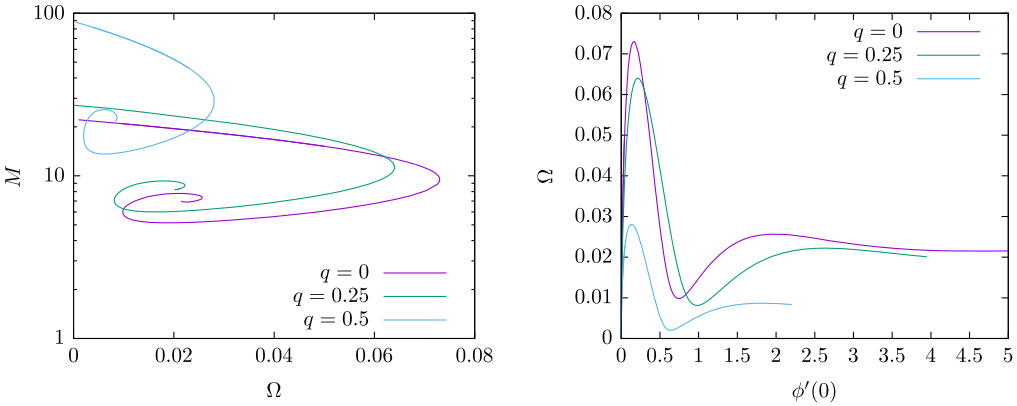


FIG. 2. Mass $M$ in dependence of $\Omega$ (left) and $\Omega$ in dependence of $\phi'(0)$ (right) for EM boson stars with $q = 0.25$ (purple) and $q = 0.5$ (green), respectively. For comparison, we also show the uncharged case, $q = 0$.

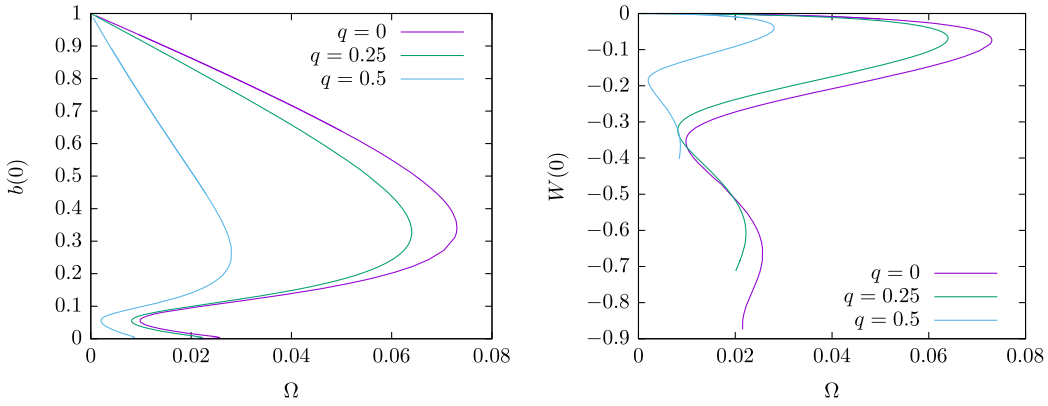


FIG. 3. Value of the metric function $b(r)$ at the origin, $b(0)$ in dependence of $\Omega$ (left), and the value of the metric function $W(r)$ at the origin, $W(0)$ in dependence of $\Omega$ (left) for EM boson stars with $q = 0.25$ (purple) and $q = 0.5$ (green), respectively. For comparison, we also show the uncharged case, $q = 0$.

minimal value and, for sufficiently large $\phi'(0)$, tends to a constant value of $\Omega$. The solutions cease to exist when $\phi'(0)$ is too large, where the maximal possible value of $\phi'(0)$ decreases with increasing $q$. This is related to the formation of a singularity in the Ricci scalar at the origin. The Ricci scalar at $r = 0$ is given by $\mathcal{R}(0) = -4b''(0)/b(0) - 6f''(0)$ [compare (28)]. In Fig. 3 (left) we show the value of $b(0)$ in dependence of $\Omega$ for $q = 0$, $q = 0.25$, and $q = 0.5$. For $\Omega = 0$ we find $b(0) = 1$ independent of $q$ as this is the limit of the vanishing scalar field $\phi(r) \equiv 0$. Along the branches, i.e., increasing $\phi'(0)$, the value of $b(0)$ decreases until it reaches zero; i.e., a solution with a diverging Ricci scalar at $r = 0$ is reached. We also observe that $W(0)$ decreases from zero when moving along the branches; see Fig. 3 (right). In particular, we find that $g_{tt} = -b + hW^2$ can become zero and even positive, indicating that an ergoregion exists for solutions with sufficiently large $\phi'(0)$. As has been discussed in the context of boson stars before [7], this would make the solutions unstable. We find that the larger $q$, the smaller the value of $\phi'(0)$ at which an ergoregion appears; e.g., for $q = 0.25$, we find solutions with ergoregions for $\phi'(0) > 1.2$, while these ergoregions exist for $\phi'(0) > 0.9$ when choosing $q = 0.5$. Some data are shown in Table I, where we give the two values of $r$ at which $g_{tt}$ becomes zero. The ergoregion is a hyperspherical shell of inner radius $r_1$ and outer radius $r_2$. Within this shell, $g_{tt}$ is positive and attains its maximal value at $r^{(\max)}$. The maximal value of $g_{tt}$ and the value of $r^{(\max)}$ are also given in Table I.

TABLE I. Two values of $r$ for which $g_{tt}$ becomes zero. The inner radius $r_1$ and outer radius $r_2$, respectively, of the ergoregion, as well as the value of $r = r^{(\max)}$ at which $g_{tt}$ attains its maximal value $g_{tt}^{(\max)}$, are given for EM boson stars and some values of $\phi'(0)$ and $q$.

| $\phi'(0)$ | $q$ | $r_1$ | $r_2$ | $r^{(\max)}$ | $g_{tt}^{(\max)}$ |
|---|---|---|---|---|---|
| 1.6 | 0.25 | 0.29 | 0.97 | 0.75 | 0.038 |
| 1.2 | 0.25 | 0.64 | 0.91 | 0.84 | 0.007 |
| 1.6 | 0.5 | 0.22 | 1.14 | 0.79 | 0.033 |
| 1.0 | 0.5 | 0.66 | 1.18 | 0.90 | 0.008 |
| 0.95 | 0.5 | 0.76 | 1.14 | 0.96 | 0.004 |

In Fig. 4 we show the gauge field energy density $\epsilon_v$ and scalar field energy density $\epsilon_s$ given by

$$\epsilon_v \equiv (T_0^0)_v = \frac{f}{2bh}(A')^2(b - hW^2) + \frac{2}{r^4}A^2 + \frac{f}{2b}(V')^2 \tag{29}$$

and

$$\epsilon_s \equiv (T_0^0)_s = f(\phi')^2 + \mu^2\phi^2 + \phi^2\left(\frac{2}{r^2} + \frac{(1 - qA)^2}{h}\right) + \frac{\phi^2}{b}((qV - \omega)^2 - W^2(qA - 1)^2), \tag{30}$$

respectively. The sum $\epsilon_v + \epsilon_s$ is equivalent to the total energy density of the solution. These profiles are for $q = 0.5$ and $\phi'(0) = 0.8$ (left) and $\phi'(0) = 1.6$ (right), respectively. We also show the metric tensor component $-g_{tt}$. We observe that the scalar field energy density $\epsilon_s$ dominates the energy density as it is a factor of 50 larger than the contribution $\epsilon_v$ from the gauge field. The gauge field energy density $\epsilon_v$ is maximal at the center of the boson star, while $\epsilon_s$ has its maximal value at $r = r_{s,\max} > 0$. Interestingly, the gauge field energy density, as well as $-g_{tt}$, has a local minimum around $r_{s,\max}$. For sufficiently large scalar field energy density, we find that $-g_{tt}$ becomes negative; i.e., an ergoregion appears. Increasing $\phi'(0)$ from 0.8 to 1.6 leads to an increase of $\Omega$; i.e., the scalar field falls off more quickly. Correspondingly, $r_{s,\max}$ decreases, and the maximum of the energy density increases with increasing $\phi'(0)$.

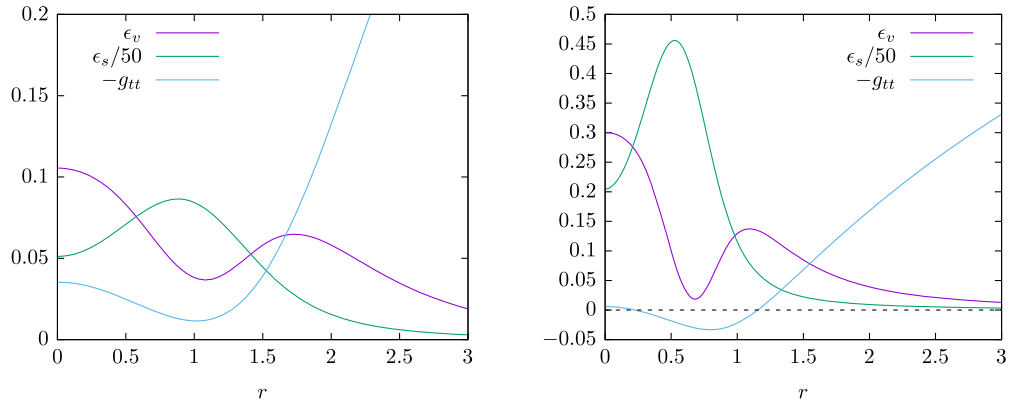


FIG. 4. Profiles of the gauge field energy density $\epsilon_v$, the scalar field energy density $\epsilon_s$, and the metric function $-g_{tt}$ for EM boson stars with $q = 0.5$, $\gamma = 0$ and $\phi'(0) = 0.8$ (left) and $\phi'(0) = 1.6$ (right).

We also studied the gyromagnetic ratio for the solutions. Our results for $q = 0.25$ and $q = 0.5$ are shown in Fig. 5 (left). On the main branch for $\Omega \to 0$, the gyromagnetic ratio tends to the "classical" value $\gamma = 1$. Increasing $\Omega$ from zero leads to an increase in $\gamma$ up to a maximal value on the second branch of solutions. The larger $q$, the larger this maximal value.

In order to better understand the dependence of the solutions on $\phi'(0)$ and $q$, we also studied the case of fixed $\phi'(0)$ and varying $q$. Our numerical experiments indicate that localized solutions do not exist for $q > q_{\max}$ with $q_{\max} \approx 0.5775$ more or less independent of the choice of $\phi'(0) > 0$. This is shown in Fig. 6 (left) where we give $\Omega$ as a function of $q$ for three different values of $\phi'(0)$. Obviously, when $q \to q_{\max}$ the value of $\Omega \to 0$; i.e., the boson star solution is no longer (exponentially) localized. Accordingly, all physical quantities subject to a Gauss law (mass $M$, electric charge $Q_e$, magnetic moment $Q_m$, angular momentum $J$) will diverge in this limit. However, it is interesting to note that the gyromagnetic ratio $\gamma$ behaves differently in the limit $q_{\max} \approx 0.5775$ when choosing $\phi'(0)$ to be small instead of large. This is shown in Fig. 6 (right) where we give $\gamma$ as a function of $q$ for different values of $\phi'(0)$. We observe that for small values of $\phi'(0)$ [here, $\phi'(0) = 0.035$], the gyromagnetic ratio increases strongly for $q \to q_{\max}$, while for large values of $\phi'(0)$ [here, $\phi'(0) = 1.6$ and $\phi'(0) = 3.7$, respectively], $\gamma$ decreases strongly in this limit. Note that this limit for $q$ was also observed for the corresponding black hole solutions [18].

### B. Einstein-Maxwell-Chern-Simons boson stars

In the following, we discuss the influence of the CS term on the properties of the charged boson stars. As expected, the EM boson stars are progressively deformed when choosing $\alpha \neq 0$. As an example we show the dependence of the mass $M$ and the angular momentum $J$ (left)—as well as the electric charge $Q_e = Q$, the magnetic moment $Q_m$, and the value of the electric potential at infinity

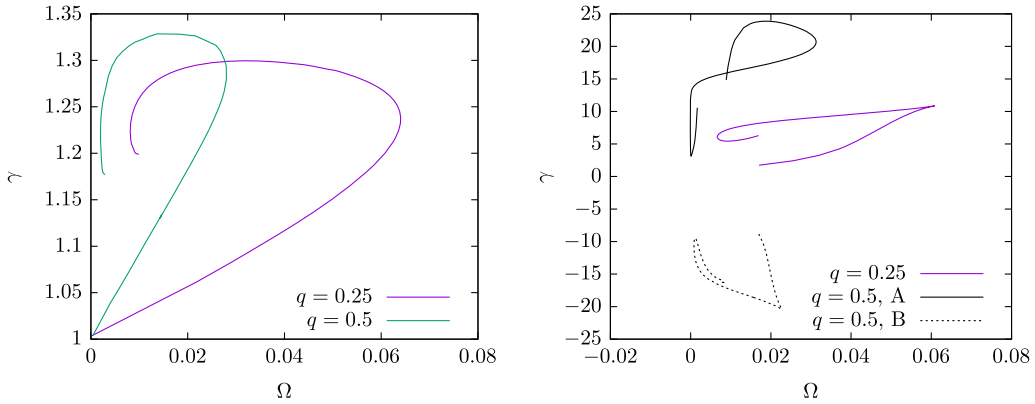


FIG. 5. Left panel: gyromagnetic ratio $\gamma$ in dependence of $\Omega$ for EM boson stars with $q = 0.25$ (purple) and $q = 0.5$ (green), respectively. Right panel: gyromagnetic ratio $\gamma$ in dependence of $\Omega$ for EMCS boson stars with $\alpha = 1$ and $q = 0.25$ (purple) and $q = 0.5$ (black), respectively. In the latter case, we show branch A (solid) and branch B (dashed), respectively.

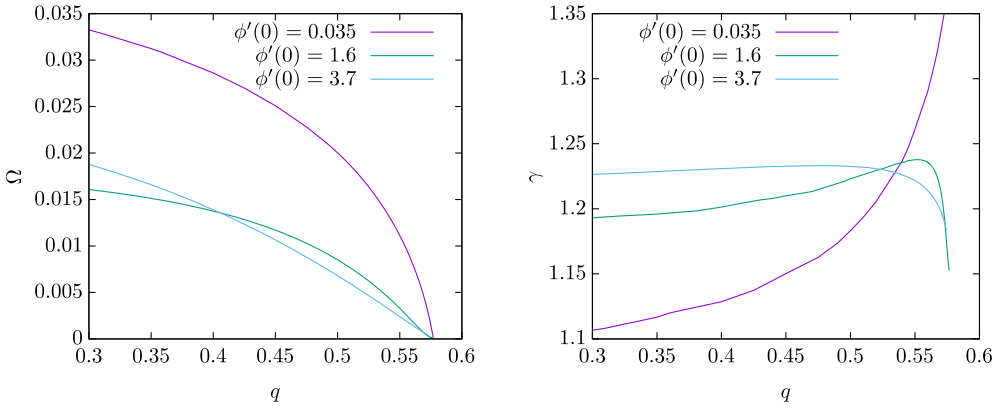


FIG. 6. Left panel: value of $\Omega$ in dependence of $q$ for EM boson stars with $\phi'(0) = 0.035$ (purple), $\phi'(0) = 1.6$ (green), and $\phi'(0) = 3.7$ (blue), respectively. Right panel: gyromagnetic ratio $\gamma$ in dependence of $q$ for the same solutions.

$V_\infty$ (right)—on $\alpha$ for $\phi'(0) = 0.35$ and $q = 0.5$ in Fig. 7. As these figures suggest, two branches of solutions exist, which we refer to as "branch A" and "branch B" in the following. Branch A is connected to the EM limit $\alpha \to 0$ and exists for both positive and negative values of $\alpha$, while branch B appears only for sufficiently large and positive values of $\alpha$, i.e., for $\alpha > \alpha_{\mathrm{cr,B}}$, where $\alpha_{\mathrm{cr,B}}$ depends on $q$ and $\phi'(0)$. For $q = 0.5$ and $\phi'(0) = 0.35$ we find that $\alpha_{\mathrm{cr,B}} \approx 0.405$.

Solutions on both branches have the feature that $M > J$, and both $M$ and $J$ decrease with increasing $\alpha$ (except close to $\alpha_{\mathrm{cr,B}}$ on branch B where our numerical results indicate an increase on a small interval of $\alpha$).

The results suggest that mass and angular momentum of the solutions on branch A change little when increasing $\alpha$ from negative values to zero. Even for small positive values of $\alpha$, this seems to be the case. For slightly smaller $\alpha$, but close to $\alpha_{\mathrm{cr,B}}$, we find that $M$ and $J$ drop sharply and then, on a large interval of (positive) $\alpha$, remain nearly constant. This suggests that the appearance of branch B seems to be connected to a drop in energy and angular momentum of the boson stars on branch A. All our numerical results indicate that these two branches remain separated and do not merge at sufficiently large $\alpha$. We also observe that the electric charge $Q_e = Q$ decreases with increasing $\alpha$ for both branches [see Fig. 7 (right)] with $Q_e = Q$ smaller on branch A as compared to on branch B. Note that $|V_\infty|$ decreases with increasing $\alpha$ and is again larger on branch B. Finally, the magnetic moment $Q_m$ is close to zero for negative $\alpha$ (branch A) and increases to positive values when increasing $\alpha$ from zero. On branch B, the magnetic moment is negative and decreases in absolute value when increasing $\alpha$ and approaches zero for large positive values of $\alpha$. The solutions on branch B hence have larger electric charge and larger absolute value of the magnetic moment, with the latter being negative on branch B. In order to understand the difference between the two branches, we have plotted the profiles of typical boson star solutions. This is shown in Fig. 8 (left) for $q = 0.5$, $\alpha = 0.5$, and $\phi'(0) = 0.35$.

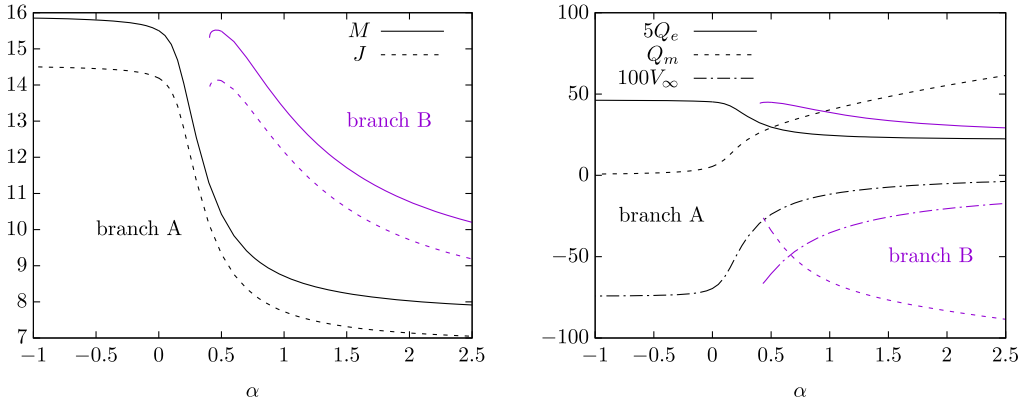


FIG. 7. Mass $M$ and angular momentum $J$ (left) and the electric charge $Q_e = Q$, the magnetic moment $Q_m$, and the value of the electric potential at infinity $V_\infty$ (right) of EMCS boson stars in dependence of $\alpha$ for $\phi'(0) = 0.35$ and $q = 0.5$. We show branch A with no node (black) and branch B with one node (violet) of the gauge field function $A(r)$; see also Fig. 8.

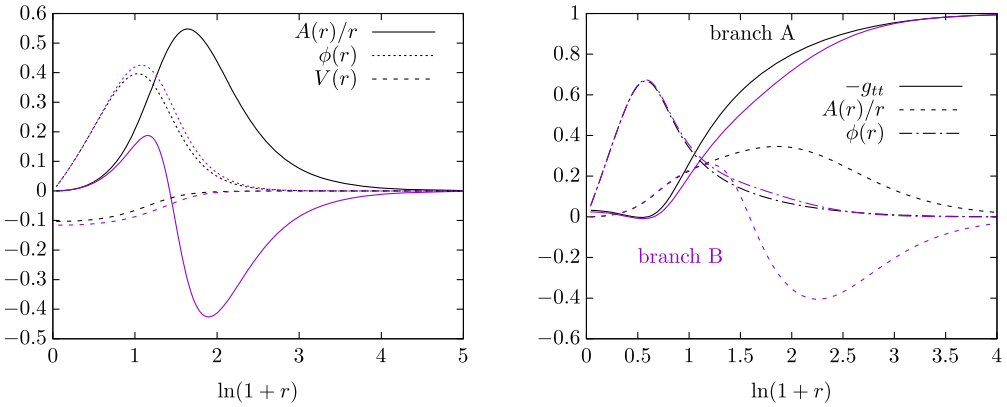


FIG. 8. Left panel: profiles of the gauge potential functions $A(r)/r$ (solid) and $V(r)$ (dashed) as well as of the scalar field function $\phi(r)$ (dotted) for EMCS boson stars on branch A (black) and branch B (violet) for $q = 0.5$, $\alpha = 0.5$, and $\phi'(0) = 0.35$. Right panel: metric tensor component $-g_{tt}$ (solid), gauge potential function $A(r)/r$ (dashed), and scalar field function $\phi(r)$ (dotted-dashed) for EMCS boson stars on branch A (black) and branch B (violet) for $q = 0.5$, $\alpha = 0.5$, and $\phi'(0) = 1.3$.

Clearly, the magnetic potential $A(r)$ possesses a node for the solutions on branch B. Solutions with nodes in the spatial part of the gauge field have been found before for black holes in EMCS theory (without scalar fields) [15]. These have been interpreted as radial excitations, and the fact that solutions on branch B have larger mass than those on branch A suggests that this interpretation is also suitable here. Interestingly, we observe that neither the electric part of the gauge potential [given in terms of the function $V(r)$] nor the scalar field function $\phi(r)$ is strongly changed when radially exciting the magnetic part of the gauge potential. Fixing $q$ and $\alpha$ and increasing $\phi'(0)$ we find that the value of $r = r_0$ at which $A(r)$ becomes zero increases. This is shown in Fig. 8 (right) for $\phi'(0) = 1.3$. In this case we find that for $0 \leq r \lesssim r_0$ the solutions on the two branches barely differ from each other. This includes the extent and existence of the ergoregion, which is slightly more extended for solutions on branch B; see also Table II for more data. These data also suggests that at fixed $\phi'(0)$ and fixed $q$, the ergoregion has smaller radial thickness when the CS term is present.

The solutions on branch B possess negative magnetic moments and hence negative gyromagnetic ratios. Our results for $\alpha = 1$ and $q = 0.25$ as well as $\alpha = 1$ and $q = 0.5$ on branch A and branch B are shown in Fig. 5 (right).

TABLE II. Two values of $r$ for which $g_{tt}$ becomes zero, i.e., the inner radius $r_1$ and outer radius $r_2$, respectively, of the ergoregion for EMCS boson stars with $q = 0.5$ and some exemplary values of $\phi'(0)$ and $\alpha$.

| $\phi'(0)$ | $\alpha$ | $r_1$ | $r_2$ | Branch |
|---|---|---|---|---|
| 1.6 | 0.5 | 0.33 | 0.87 | A |
| 1.6 | 0.5 | 0.31 | 0.93 | B |
| 1.3 | 1.0 | 0.59 | 0.80 | A |
| 1.2 | 1.0 | 0.60 | 0.87 | B |

In comparison to the EM case, the gyromagnetic ratio can become negative (branch B for $q = 0.5$) and significantly larger in absolute value. The maximal possible value of $\gamma$ increases with $q$ and is an order of magnitude larger compared to the EM boson stars.

When plotting the mass $M$ as a function of $\Omega$ [see Fig. 9 (left)], we find that the maximal possible value of $\Omega$ increases with increasing $\alpha$ and that, on the second branch, the solutions exist down to $\Omega \approx 0$ where a third branch of solutions emerges, showing a sharp increase in mass $M$ on a very small interval of $\Omega$. Reaching a maximal mass, a fourth branch emerges on which the mass decreases again. We find that the larger $\alpha$, the sharper the increase of the mass on the third branch. Comparing the solutions on branch A and branch B for $\alpha = 1$, we find that the qualitative dependence of the mass on $\Omega$ is quite different. In particular, we notice that the qualitative dependence of the solutions on branch B for $\alpha = 1$ seems similar to that of the solutions for $\alpha = 0.5$. Finally, we checked the dependence of the magnetic moment $|Q_m|$ on the angular momentum $J$ of the solutions. This is shown in Fig. 9 (right). Interestingly, we find a nearly linear relation between $\log|Q_m|$ and $\log J$ on the first two branches of solutions, where the first branch has a larger slope than the second. The third and fourth branches show more complicated behavior. This relation was found before from observations of planets and stars [21]. While boson stars are assumed to be very compact objects and hence rather comparable in density to neutron stars and white dwarfs, our results suggest that (at least in five dimensions) EMCS boson stars have the property that $Q_m$ is proportional to a positive power of $J$, i.e., that $Q_m$ would increase when $J$ increases. This seems to be different for neutron stars and white dwarfs which have $Q_m$ proportional to a negative power of $J$ [21], and hence the magnetic moment would decrease with increased angular momentum.

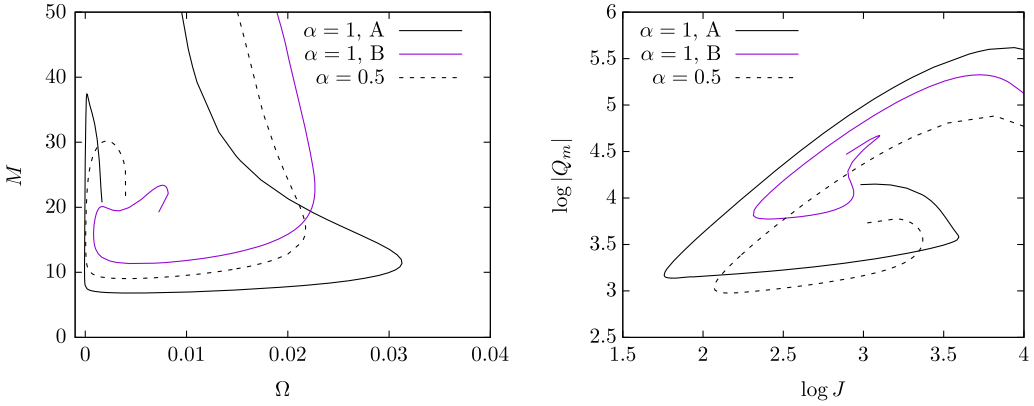


FIG. 9. Left panel: mass $M$ as a function of $\Omega$ for $q = 0.5$ and $\alpha = 1$ (solid)—branch A (black) and branch B (violet)—as well as for $\alpha = 0.5$ (dashed). Right panel: magnetic moment $|Q_m|$ as a function of the angular momentum $J$ for the same EMCS boson stars.

## IV. CONCLUSIONS

In this paper, we have discussed the construction of charged and rotating boson stars in five space-time dimensions. The gauge field dynamics is either of Maxwell type or of Maxwell-Chern-Simons type. These solutions possess electric charge $Q$ equal to $q$ times the Noether charge $N$, where $q$ is the gauge coupling, and the sum of the two angular momenta $J$ equal to the Noether charge, i.e., $Q/q = N = J$. The gyromagnetic ratio of the solutions is on the order of unity for boson stars in standard Maxwell gauge field theory, while it can become an order of magnitude larger when the Chern-Simons interaction is added. Moreover, we observe that the presence of the Chern-Simons term leads to the existence of solutions with a radially excited magnetic gauge field component. This leads to the reversal of the sign of the magnetic moment and the gyromagnetic ratio; i.e., we find solutions with positive and negative gyromagnetic ratios in the presence of the Chern-Simons term.

For sufficiently compact boson stars we find that the space-time possesses an ergoregion which suggests that these solutions eventually become unstable. The presence of the CS term decreases the radial extension of the ergoregion at fixed $q$ and $\phi'(0)$.

When considering the relation between the magnetic moment and the angular momentum, we find a positive correlation for the solutions on the first and second branches; i.e., the absolute value of the magnetic moment increases with angular momentum. This is different for neutron stars and white dwarfs for which a negative correlation seems to exist; see, e.g., Ref. [21]. Positive correlations are typical for planets and ordinary stars. It would be interesting to investigate this question further in other space-time dimensions.

In this paper, we have discussed solutions with nodes in the gauge field function which exist only when the Chern-Simons term is present in the model. There also exist charged boson stars with nodes in the scalar field function; see, e.g., Ref. [22]. We have not attempted to construct them, but we believe that they also exist in our model.

[1] D. J. Kaup, Klein-Gordon Geon, Phys. Rev. **172**, 1331 (1968).
[2] R. Friedberg, T. D. Lee, and Y. Pang, Mini-soliton stars, Phys. Rev. D **35**, 3640 (1987).
[3] P. Jetzer, Boson stars, Phys. Rep. **220**, 163 (1992).
[4] F. E. Schunck and E. W. Mielke, General relativistic boson stars, Classical Quantum Gravity **20**, R301 (2003).
[5] B. Kleihaus, J. Kunz, and M. List, Rotating boson stars and Q-balls, Phys. Rev. D **72**, 064002 (2005).
[6] B. Kleihaus, J. Kunz, M. List, and I. Schaffer, Rotating boson stars and Q-balls. II. Negative parity and ergoregions, Phys. Rev. D **77**, 064025 (2008).
[7] V. Cardoso, P. Pani, M. Cadoni, and M. Cavaglia, Ergoregion instability of ultracompact astrophysical objects, Phys. Rev. D **77**, 124044 (2008).
[8] P. Jetzer and J. J. van der Bij, Charged boson stars, Phys. Lett. B **227**, 341 (1989).
[9] B. Kleihaus, J. Kunz, C. Lämmerzahl, and M. List, Charged boson stars and black holes, Phys. Lett. B **675**, 102 (2009).
[10] D. Pugliese, H. Quevedo, J. A. Rueda H., and R. Ruffini, On charged boson stars, Phys. Rev. D **88**, 024053 (2013).
[11] Y. Brihaye, T. Caebergs, and T. Delsate, Charged-spinning-gravitating Q-balls, arXiv:0907.0913.

[12] L. G. Collodel, B. Kleihaus, and J. Kunz, Structure of rotating charged boson stars, Phys. Rev. D **99**, 104076 (2019).
[13] B. Hartmann, B. Kleihaus, J. Kunz, and M. List, Rotating boson stars in 5 dimensions, Phys. Rev. D **82**, 084022 (2010).
[14] J. Kunz and F. Navarro-Lerida, $D = 5$ Einstein-Maxwell-Chern-Simons Black Holes, Phys. Rev. Lett. **96**, 081101 (2006).
[15] J. L. Blázquez-Salcedo, J. Kunz, F. Navarro-Lérida, and E. Radu, Radially excited rotating black holes in Einstein-Maxwell-Chern-Simons theory, Phys. Rev. D **92**, 044025 (2015).
[16] J. Kunz, J. L. Blazquez-Salcedo, F. Navarro-Lerida, and E. Radu, Einstein-Maxwell-Chern-Simons black holes, J. Phys. Conf. Ser. **942**, 012003 (2017).
[17] J. L. Blazquez-Salcedo, J. Kunz, F. Navarro-Lerida, and E. Radu, New black holes in $D = 5$ minimal gauged supergravity: Deformed boundaries and frozen horizons, Phys. Rev. D **97**, 081502 (2018).
[18] Y. Brihaye and L. Ducobu, Spinning-charged-hairy black holes in 5D Einstein gravity, Phys. Rev. D **98**, 064034 (2018).
[19] R. C. Myers and M. J. Perry, Black holes in higher dimensional space-times, Ann. Phys. (N.Y.) **172**, 304 (1986).
[20] U. Ascher, J. Christiansen, and R. D. Russell, A collocation solver for mixed order systems of boundary value problems, Math. Comput. **33**, 659 (1979); Collocation software for boundary-value ODEs, ACM Trans. **7**, 209 (1981).
[21] C. N. Arge, D. J. Mullan, and A. Z. Dolginov, Magnetic moments and angular momenta of stars and planets, Astrophys. J. **433**, 795 (1995).
[22] Y. Brihaye, B. Hartmann, and J. Riedel, Self-interacting boson stars with a single Killing vector field in anti-de Sitter space-time, Phys. Rev. **92**, 044049 (2015).